ELSEVIER

Biophysical Chemistry 103 (2003) 213–222

Biophysical Chemistry

www.elsevier.com/locate/bpc

# Correlation between fluidising effects on phospholipid membranes and mitochondrial respiration of propofol and *p*-nitrosophenol homologues

Federico Momo[a,b,*], Sabrina Fabris[a], Anna Wisniewska[c], Cristina Fiore[a], Alberto Bindoli[d], Guido Scutari[e], Roberto Stevanato[a]

[a]*Department of Physical Chemistry, University of Venice, Dorsoduro 2137, 30123 Venice, Italy*
[b]*Istituto Nazionale Fisica della Materia, Genova, Italy*
[c]*Institute of Molecular Biology and Biotechnology, Jagiellonian University, Krakow, Poland*
[d]*CNR Centre for the Study of Biomembranes, Padova, Italy*
[e]*Department of Biological Chemistry, University of Padova, Padova, Italy*

Received 25 July 2002; received in revised form 3 September 2002; accepted 3 September 2002

**Abstract**

Nitrosopropofol (2-6-diisopropyl-4-nitrosophenol) has dramatic consequences for respiration, ATP synthesis and the transmembrane potential of isolated rat liver mitochondria at concentrations at which propofol (2-6-diisopropyl-phenol) does not cause any apparent effects. These results correlate well with the observation that nitrosopropofol is also a stronger perturbing agent of phospholipid membranes. In this paper we verify the possible biological activity of different phenols and nitrosophenols on mitochondrial respiration. We then discuss their interactions with phospholipid liposomes, studied with differential scanning calorimetry, spin labelling techniques and UV-Vis spectrophotometry, in order to obtain information on drug distribution and the modifications they impose on lipid bilayer. The results of the experiments performed on mitochondria and model membranes prove an interesting correlation between the effects of the molecules on both systems.


*Keywords:* Propofol; Nitrosopropofol; Nitrosophenols; Phospholipid membrane

## 1. Introduction

Propofol (2,6-diisopropylphenol; Di-PrP) is a widely used anaesthetic, for which action on the resting and ADP-stimulated respiration, the respiratory control ratio, ATP synthesis, and the formation and utilisation of electrochemical transmembrane potential of isolated rat liver mitochondria is enhanced by the synergic presence of nitrosoglutathione (GSNO) [1].

These observations suggested that the effects might be ascribed to a new molecule, and, in a recent paper concerning the interaction between Di-PrP and GSNO, we demonstrated the formation of 2,6-diisopropyl-4-nitrosophenol (Di-PrPNO) as

*Corresponding author. Tel.: +39-041-2348599; fax: +39-041-2348594.
*E-mail address:* momo@unive.it (F. Momo).

0301-4622/03/$ - see front matter © 2002 Elsevier Science B.V. All rights reserved.
PII: S0301-4622(02)00256-9

a product of the reaction between the two compounds [2].

Di-PrPNO proved to be a stable compound with a p$K_a$ value of 7.5, much lower than the p$K_a$ of ~10.5 for Di-PrP and surprisingly near the physiological pH value.

Tested on mitochondria, Di-PrPNO is able to impair their energetic system at concentrations far lower than those required by the combination of Di-PrP and GSNO [3], so a reasonable hypothesis is that mitochondria are able to catalyse the reaction between GSNO and Di-PrP, and that this new metabolite is responsible for the reported effects on mitochondria.

Moreover, differential scanning calorimetry (DSC) and electron spin resonance (ESR) experiments on phosphatidylcholine multilamellar liposomes showed that Di-PrPNO is a stronger perturbing agent of phospholipid membranes when compared with Di-PrP [2]. Thus, the overall results indicate that the NO group attached to the Di-PrP molecule might play a crucial role, and that, most likely, the action of Di-PrPNO has to be ascribed to derangement of the membrane.

In this paper the study was extended to a series of 2,6-dialkylphenol compounds, and their 2,6-dialkyl-4-nitrosophenol derivatives, as reported in Table 1, in order to determine if other homologues of Di-PrPNO have relevant effects on the mitochondrial respiratory chain, and whether they depend or not on the presence of the NO group and of the aliphatic residues in the 2 and 6 positions. We discuss in detail the interaction of these compounds, of different steric hindrances and polarities, with phospholipid membranes, to obtain information about their distribution inside the lipid bilayer and how they interfere with the ordered lipid organisation. The investigation was performed with different techniques, such as differential scanning calorimety, spin labelling and UV-Vis spectrophotometry, which furnished useful elements in understanding the mechanisms of interaction and a possible explanation of the peculiar role of the NO group. Moreover, the results confirm tight correlation between the action of these molecules on mitochondria and their perturbing effects on membranes, thus suggesting a hypothesis that the membrane effects may be responsible for the anaesthetic action of propofol [2–4], as was already hypothesised for other classes of anaesthetics, narcotics and antidepressants [5–8].

## 2. Materials and methods

### 2.1. Chemicals

All chemicals, of the highest available quality, were obtained from Sigma Chemical Co (St. Louis,

Table 1
List of the dopants

| | | |
|---|---|---|
| 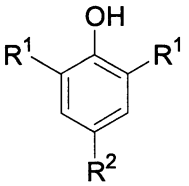 | a: $R^1$=H, $R^2$=H | phenol |
| | b: $R^1$=Me, $R^2$=H | 2,6-dimethylphenol (DMeP) |
| | c: $R^1$=*i*-Pr, $R^2$=H | 2,6-diisopropylphenol (D*i*-PrP) |
| | d: $R^1$=*t*-Bu, $R^2$=H | 2,6-ditertbutylphenol (D*t*-BuP) |
| | e: $R^1$=Me, $R^2$=NO | 2,6-dimethyl-4-nitrosophenol (DMePNO) |
| | f: $R^1$=*i*-Pr, $R^2$=NO | 2,6-diisopropyl-4-nitrosophenol (D*i*-PrPNO) |
| | g: $R^1$=*t*-Bu, $R^2$=NO | 2,6-ditertbutyl-4-nitrosophenol (D*t*-BuPNO) |

USA), while the solutions were prepared with MilliQ quality water.

### 2.2. Synthesis of nitrosophenols

The synthesis of 2,6-dialkyl-4-nitrosophenol was carried out following the same procedure as for nitrosophenol [9]. In particular, 2 ml of concentrated hydrochloric acid was slowly added to a solution of 3 g of 2,6-dialkylphenol in 25 ml of ethanol cooled to −5 °C. A solution of 1.1 g of sodium nitrite dissolved in 5 ml water was gradually added to the mixture under vigorous agitation, maintaining the temperature below 0 °C. After the addition of all the nitrite, taking approximately 15 min, the yellow product was agitated for 30 min and then poured into iced water. The yellow precipitate was crystallised from toluene and characterised by GC/MS analysis. A purity grade higher than 95% was confirmed by thin layer chromatography.

### 2.3. Liposome preparation

Multilamellar vesicles were prepared following the method of Kusumi et al. [10]. Phospholipids were dissolved in a 2:1 chloroform/methanol mixture, then dried with a stream of nitrogen gas and kept under vacuum for at least 14 h. The dried lipids were suspended, when not otherwise specified, in 0.1 M HEPES buffer, pH 7.2. The lipid dispersion, at a final lipid concentration of 101 mM, was warmed at approximately 40 °C, mixed vigorously with a vortex for 30 s and used as obtained for DSC measurements. When required, spin labels were added to the chloroform/methanol phospholipid mixture.

Unilamellar liposomes were prepared by combining freeze–thawing and extrusion protocols [11], starting from 500 μl of a 40 mM phospholipid suspension. Extrusion was performed using the Avestin Liposofast apparatus, with 100-nm-pore-size filters.

### 2.4. UV-Vis spectroscopy

Spectrophotometric measurements were recorded on a UV-Vis Beckman DU 640 instrument equipped with a thermostatted quartz cell.

### 2.5. DSC measurements

Calorimetric measurements were performed on a Setaram DSC 92 apparatus.

Approximately 50 mg of phospholipid dispersion was placed in an aluminium crucible. An identical crucible was filled with an equivalent weight of HEPES solution and placed in the reference cell.

The temperature scanning rate was 0.5 °C $min^{-1}$. The transition temperature $T_c$ from the $L_\beta$ to $L_\alpha$ phase of DMPC was taken at the peak of the DSC profiles.

### 2.6. ESR measurements

ESR measurements were performed on a Bruker ESP300E 9-GHz spectrometer at 10 mW of microwave power. Samples were placed in a gas-permeable TPX tube of 1 mm i.d. (Wilmad, NJ, USA) and centred in the resonant cavity, then deoxygenated under nitrogen flow above $T_c$ for 10 min.

ESR spectra are interpreted in terms of $A_{max}$, the separation between the outer hyperfine lines.

### 2.7. Mitochondria preparation

Mitochondria were isolated from liver of albino Wistar rats in 0.25 M sucrose, 10 mM Na–HEPES (pH 7.4), and 0.25 mM EGTA by differential centrifugation, omitting EGTA in the final washing. Protein content in the mitochondrial suspension was assayed by the biuret method [12]. All experiments were carried out at 20 °C using 1 mg of mitochondrial protein $ml^{-1}$ of a basal medium containing 0.25 M sucrose, 15 mM MOPS, 1.5 μM rotenone, 1.6 mM $MgSO_4$, 2 mM $KH_2PO_4$, 6 mM NaCl and 1 mg $ml^{-1}$ BSA, pH 7.0. Oxygen consumption was followed using a Clark oxygen electrode (Yellow Springs Instruments Co) in the basal medium supplemented with 5 mM potassium succinate and 1.5 μM rotenone (final volume 1.6 ml).

## 3. Results and discussion

### 3.1. Mitochondria respiration rates

The effects of phenol, dimethylphenol, diisopropylphenol and di*tert*butylphenol and of their *para*-

Table 2
Oxygen consumption of isolated rat liver mitochondria in the presence of 2,6-dialkyl-phenols and nitrosophenols

| | Control | Phenol | DMeP | Di-PrP | D*t*-BuP | DMePNO | Di-PrPNO | D*t*-BuPNO |
|---|---|---|---|---|---|---|---|---|
| State 3 | 44±3 | 42±3 | 45±4 | 41±3 | 45±3 | 35±4 | 32±4 | 38±5 |
| State 4 | 10±2 | 14±2 | 13±2 | 14±1 | 16±2 | 16±2 | – | – |
| RCR | 4.2±0.4 | 2.8±0.5 | 3.1±0.5 | 2.7±0.2 | 3±0.3 | 2.3±0.7 | – | – |
| CCCP | 69±5 | 66±5 | 64±6 | 66±4 | 75±4 | 57±6 | 40±7 | 39±6 |

Respiration values are expressed as nmol $O_2$ $min^{-1}$ $mg^{-1}$ of mitochondrial protein ±S.D.; RCR represents the ratio between the oxygen consumption rate in the presence (state 3) and absence (state 4) of added ADP (300 nmol). CCCP indicates the oxygen consumption rate in the presence of the uncoupler carbonyl cyanide *m*-chlorophenylhydrazone (1.6 mM). Dopant concentration: 25 μM.

nitrosilated forms on the respiration rate, measured during (state 3) and after (state 4) a phosphorylation pulse induced by the addition of ADP and after the addition of the uncoupler CCCP, are reported in Table 2. The data show that the effectiveness of substituted phenols on the mitochondrial energetic metabolism is enhanced by nitrosation of the molecule and is conditioned by the structure of the alkyl groups in the 2 and 6 positions. It is indeed apparent that the presence of isopropyl and *tert*butyl groups allows the nitrosophenol to be strongly toxic to mitochondria, which are unable to respond to either a phosphorylation pulse or to the uncoupler effect. The substitution of isopropyl and *tert*butyl groups with smaller methyl groups limits the effect of nitrosophenols and leads to slowing down of the ADP-stimulated respiration and to an increase in the resting oxygen consumption rate. However, mitochondria maintain the ability to respond to ADP or CCCP stimulation, suggesting that the structure of the hydrophobic alkyl residues is a major factor in conditioning the interaction of the substituted nitrosophenols with the mitochondrial inner membrane. On the other hand, substituted but not nitrosilated phenols at the concentrations tested have a poor effect, limited to an increase in the resting respiration rate, which is an expected consequence of the interaction of a hydrophobic molecule with the mitochondrial membrane, showing that the influence of the –NO group in the phenolic structure represents an essential co-operating factor. When concentrations as low as 12.5 μM (data not reported) are adopted, nitrosilated and isopropyl- or *tert*butyl-substituted molecules are only able to induce an increase in the state-4 respiration rate, indicating a decrease in the energetic efficiency, but not dramatic impairment of the system. In addition, the oxygen consumption stimulation evoked by the uncoupler suggests that, unlike for 25 μM Di-PrPNO and D*t*-BuPNO, the structural integrity of the electron carriers is not compromised.

### 3.2. Differential scanning calorimetry

The DSC profiles of the liposomes and the plot of their transition temperature $T_c$ vs. 2,6-dialkylphenol or 2,6-dialkyl-4-nitrosophenol concentration are reported in Figs. 1–3. It is immediately evident that, according to their effect on the gel-to-fluid state transition, the molecules can be divided in two well-separated groups. All the 2,6-dialkylphenols fall into the first group, characterised by some decrease in $T_c$ and a slight broadening of the profiles at increasing dopant concentrations; all the $T_c$ values are tightly grouped around the same values, and the results can be interpreted in terms of non-polar molecules that interact non-specifically with the membrane, producing a limited decrease in the temperature and co-operativity of the transition [13]. On the basis of the calorimetric data, DMePNO has to be assigned to this group as well.

The behaviour of Di-PrPNO and D*t*-BuPNO is markedly different: both compounds lead to a stronger decrease in both the temperature and co-operativity of the transition, as demonstrated by the large broadening of the profiles, and destroy any detectable transition at concentrations less than 10 mM, while, in the presence of all other molecules, the transition is still clearly detectable.

The decrease in $T_c$ corresponds to preferred partitioning of the dopants into the liquid compared to the gel phases of DMPC [14]; for *p*-alkylphenols, it was found that the partitioning is dominated by attractive forces, which may be of van der Waals' type, or may arise from hydrogen bonding of the phenolic OH group to the phospholipid [15]. These conclusions can be reasonably extended to molecules of the first group, while the strong differences in $\Delta T_c$ observed in the case of Di-PrPNO and D*t*-BuPNO seem to imply that other forces control the interaction of these molecules with the lipid moiety.

### 3.3. ESR measurements

ESR spectra were collected for stearic acids, spin labelled at the 5th, 7th and 10th carbon positions (nSASL) and incorporated in DMPC liposomes, with and without dopants, as described in Section 2. The spectra were collected at 20.0 °C, below the gel-to-fluid state transition temperature of DMPC, because, as already observed in [2], above the transition temperature, the lipid matrices can accommodate rather high concentrations of the dopants without aggravating the disordered motions of the lipid chains. Under these experimental conditions, $A_{max}$ is a useful parameter for monitoring the effects of dopants on lipid alkyl chain order and motion [16].

The values of $A_{max}$ in the presence of various dopants at 5 mM concentration are shown in Fig. 4. With the exception of Di-PrPNO and D*t*-BuPNO, the $A_{max}$ values for a given SASL are quite similar, lying very near the unperturbed value of nSASL in pure DMPC. The results are coherent with those obtained by DSC and confirm that the molecules of the first group have very poor effectiveness on the lipid bilayer. In any case, the spin labelling technique allows better insight into the mechanisms of interaction between the dopants and DMPC membrane, showing that, at the concentrations used in these experiments, the deepest region of the bilayer is scarcely affected by the presence of the dopants, and that the major effects of Di-PrPNO and D*t*-BuPNO originate from their partitioning into the interfacial region or the hydrocarbon region, which is very close to the membrane surface.

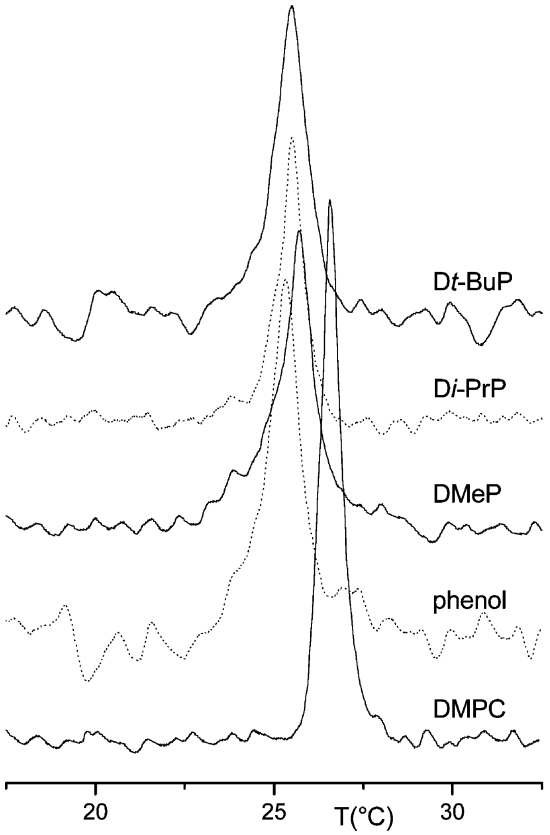


Fig. 1. DSC profiles of the gel-to-fluid state transition of DMPC multilamellar liposomes doped with 5mM 2,6-dialkylphenols: *y*-axis, d$H$/d$T$ in arbitrary units; *x*-axis, temperature $T$ in °C.

### 3.4. Monolamellar liposomes

All 2,6-dialkyl-4-nitrosophenols present two absorption bands, corresponding to their protonated (approx. 300–310 nm) and deprotonated (375–385 nm) forms. The UV-Vis spectra of the compounds in liposomes were collected after dispersing 25 μl of the liposome suspension in a spectrophotometer cell containing 975 μl of buffer thermostatted at 20 °C. The linescattering contribution to the overall absorbance was minimised by subtracting from each spectrum one obtained,

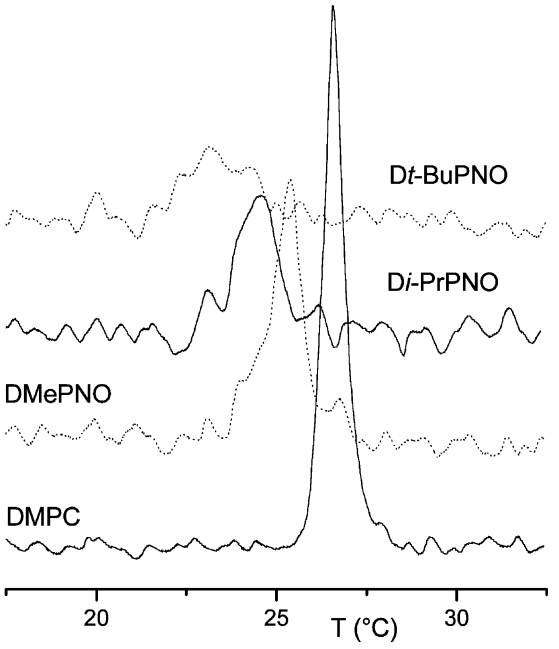


Fig. 2. DSC profiles of the gel-to-fluid state transition of DMPC multilamellar liposomes doped with 5mM 2,6-dialkyl-4-nitrosophenols.

under the same experimental conditions, from a liposomes suspension without dopants.

The experiments presented above were performed on multilamellar liposomes and were useful in establishing some clear differences between the two groups of dopants; for a more detailed analysis of the mechanisms of interaction of 2,6-dialkyl-4-nitrosophenols with the membranes, it then seemed appropriate to use monolamellar liposomes, which, under many aspects, are a more representative and suitable model of biomembranes.

The spectra of DMePNO, Di-PrPNO and D*t*-BuPNO in the buffer solution and in the liposome suspension at pH 7.2 are shown in Fig. 5.

In the spectra from liposomes, both the nitrosophenols adsorbed to the membrane, and molecules remaining free in the buffer solution contribute to the net absorbance, but their ratios cannot be unequivocally determined. In any case, it appears from Fig. 5 that the protonated fraction of dopants in the liposome suspension is always larger than in solution, indicating without ambiguity that part of the dopant concentration is withdrawn from the acid–base equilibrium of the buffer and represents protonated molecules in the lipid phase.

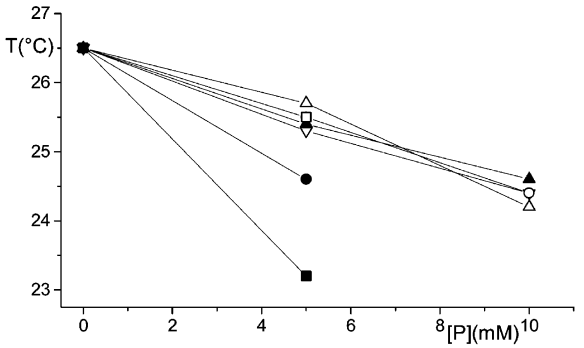


Fig. 3. Phase transition temperatures of DMPC liposomes vs. dopant concentration: ■ D*t*-BuPNO; ● Di-PrPNO; ▲ DMePNO; □ D*t*-BuP; ○ Di-PrP; Δ DMeP; ∇ phenol. The temperatures were taken at the peak of the DSC profile.

The fraction of this component (III) can be calculated by subtraction of the spectra of dopants in liposomes (I) and in pure buffer solution (II), as illustrated in Fig. 6 for Di-PrPNO. The amplitude of spectrum II subtracted from I is in some measure arbitrary, with the only upper limit that spectrum II must be lower than I at all wavelengths; to perform the difference, we used the maximum amplitude allowed for spectrum II for the three dopants. It must be stated that this does not totally coincide with the subtraction of the

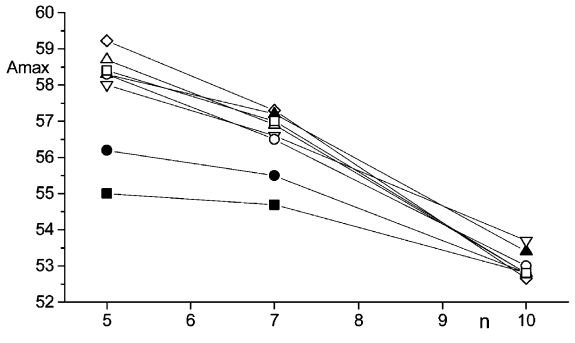


Fig. 4. $A_{max}$ values (in $10^{-4}$ T) vs. spin label position ($n$) for various dopants at 5 mM concentration: ◇ without dopants; ■ D*t*-BuPNO; ● Di-PrPNO; ▲ DMePNO; □ D*t*-BuP; ○ Di-PrP; Δ DMeP; ∇ phenol.

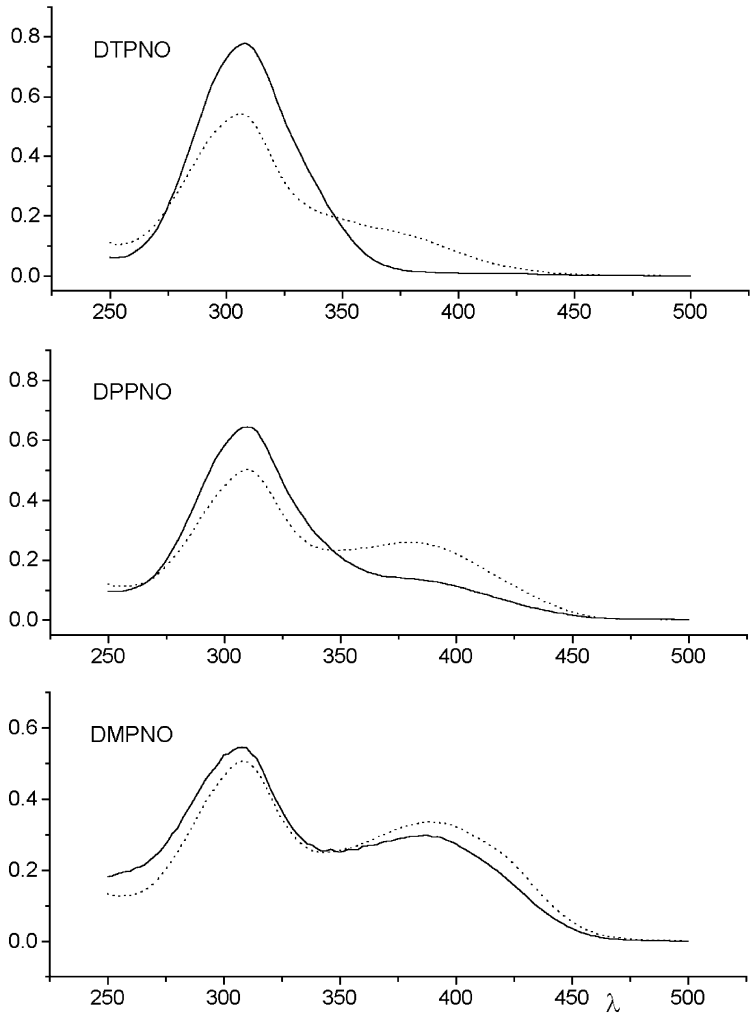


Fig. 5. UV-Vis absorption spectra of D*t*-BuPNO, Di-PrPNO and DMePNO at pH 7.2 in monolamellar liposomes (*solid line*) and pure in the buffer solution (*dotted line*): *y*-axis, absorbance; *x*-axis, wavelength in nm.

dopant concentration free in solution, because the fraction of dopant in the headgroup region is also subtracted, and which is still exposed to the acid–base equilibrium of the buffer. In our opinion, this unavoidable uncertainty cannot impair interpretation of the experimental results discussed in the following.

The fraction of the protonated component represented by spectrum III for the three dopants at pH 7.2 is plotted in Fig. 7a. To account for the different p$K_a$ values of the three molecules (DMePNO = 7.4, Di-PrPNO = 7.5, D*t*-BuPNO = 8.2), which were experimentally determined by the method reported in [2], the values of the protonated fraction at 1.3 pH units over the respective p$K_a$ value are plotted in Fig. 7b; under these conditions the dopants free in solution are almost completely deprotonated.

The graphs clearly show that the protonated component in the lipid phase is by far the most prevalent in D*t*-BuPNO, then diminishes in the order Di-PrPNO and DMePNO. The data, when interpreted together with the ESR outcomes, suggest that D*t*-BuPNO resides in the glycerol sur-

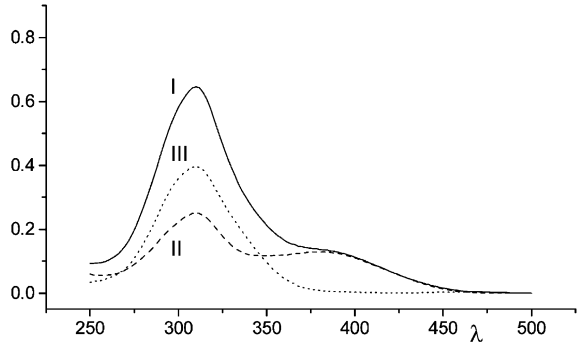


Fig. 6. Difference (III) between the UV-Vis absorption spectra of Di-PrPNO at pH 7.2 in monolamellar liposomes (I) and pure in the buffer solution (II).

roundings, while Di-PrPNO and DMePNO are more exposed to water and to the acid–base equilibrium of the buffer.

The trend corresponds to the different screening exercised on the phenolic polar OH group by the 2,6-di*tert*butyl, diisopropyl and dimethyl residues: they can be considered the structural factors that, regulating the hydrophobic character of the dopants, determine their partitioning and position inside the headgroup region. From this point of view, the alkyl groups acquire a biological relevance, because, modulating the protonated fraction, they modulate the effects on the membrane of the three molecules as well. In fact, the experiments clearly demonstrate that the variations induced on the transition temperatures and spin labelling parameters by the presence of dopants are correlated with the amount of their protonated component.

These conclusions are also confirmed by spin labelling measurements repeated on monolamellar liposomes, for which results are summarised in Fig. 8. $\Delta A_{max}$ values are the difference between the unperturbed value of $A_{max}$ in pure liposomes and in the presence of dopants, and clearly demonstrate the dependence of the perturbative effect on the pH, and consequently on the protonated fraction of the dopants. As a side note, it can be observed that a meaningful decrease in $A_{max}$ is also produced by DMePNO, but only at the lowest pH value.

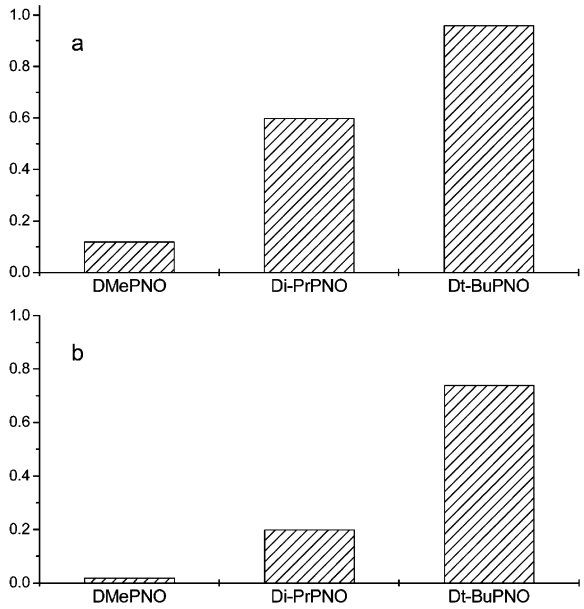


Fig. 7. Fraction of the protonated component withdrawn by the membrane from the acid–base equilibrium of the buffer: (a) in monolamellar liposomes at pH 7.2; and (b) in monolamellar liposomes at pH 8.7 (DMePNO), 8.8 (Di-PrPNO) and 9.5 (D*t*-BuPNO).

The different behaviour of 2,6-dialkylphenols with respect to 2,6-dialkyl-4-nitrosophenols remains to be discussed, given that 2,6-dialkylphenols are expected to diffuse into the membrane

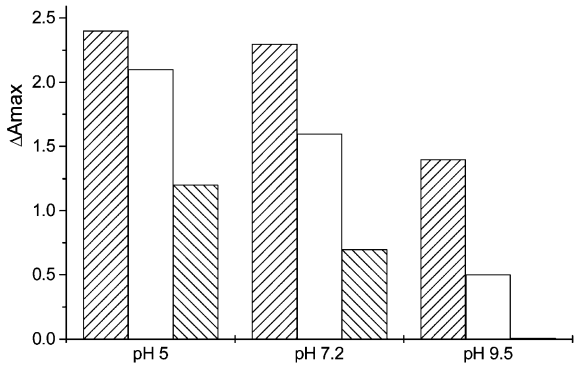


Fig. 8. $\Delta A_{max}$ values (in $10^{-4}$ T) of 5SASL in monolamellar liposomes doped with 2mM of: \\\ DMePNO; □ Di-PrPNO; and /// D*t*-BuPNO at different pH values.

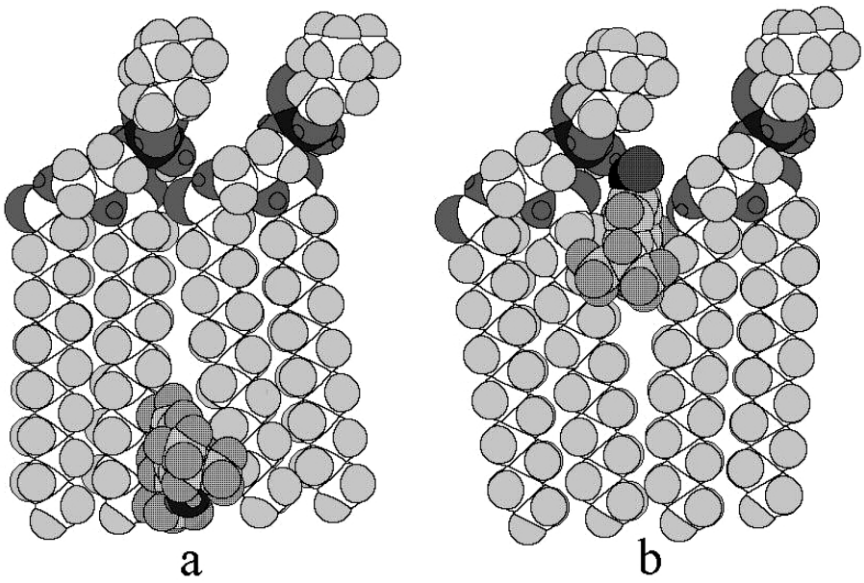


Fig. 9. Space-filling model representing the proposed disposition of dopants inside the phospholipid bilayer: (a) Di-PrP; and (b) Di-PrPNO.

even more than their nitroso analogues, due to their lower polarity.

Most likely, 2,6-dialkylphenols do not provoke meaningful modifications of the ordered disposition of phospholipids, because they are planar compounds that dispose themselves with their plane parallel to the phospholipid chains, in a configuration which minimises distortions in the chain alignment and does not greatly reduce their van der Waals' interactions.

In the model we outline, the difference is made by the presence of NO, which favours the anchoring of 2,6-dialkyl-4-nitrosophenols at the interface, and one plausible mechanism could originate from anchoring of nitrosophenols to the glycerol group through hydrogen bonds, or to the negative phosphate group through dipole–ion interactions.

A tentative suggestion of the different disposition inside the bilayers of phenols and of their nitrosilated homologues is given in Fig. 9.

## 4. Conclusions

This work is the natural progression from a previous study on propofol (Di-PrP) and nitroso-propofol (Di-PrPNO) [1–3], which stressed the enhanced action on mitochondria and model membranes of the nitroso form with respect to the commonly used anaesthetic. Extension of the study to other phenols and 2,6-dialkyl-substitued nitrosophenols has demonstrated the existence of a clear correlation between the structural factors of the molecules and their activity. In particular, the presence of the NO group is an essential requisite, and spin labelling measurements suggest that it could favour the binding of nitrosophenols inside the membranes. On the basis of the experimental observations, it also appeared that D*t*-BuPNO, based on its significant effects, could be a new molecule of pharmacological interest.

Furthermore, we expected to obtain information from this study on the mechanisms underlying the anaesthetic properties of propofol, which are still not understood. The possibility that propofol may exert its action through a non-specific interaction with the lipid moiety of biomembranes is clearly stated in [4]. Our data give support to this hypothesis, showing tight correlation between the activity of these molecules on mitochondria and their effect on phospholipid bilayers, and suggest that the

factor really responsible for the pharmacological action of propofol could be metabolic production of its nitroso form.

## References

[1] R. Stevanato, F. Momo, M. Marian, et al., Combined effect of propofol and GSNO on oxidative phosphorylation of isolated rat liver mitochondria, Nitric Oxide 5 (2001) 158–165.

[2] F. Momo, S. Fabris, A. Bindoli, G. Scutari, R. Stevanato, Different effects of propofol and nitroso propofol on DMPC multilamellar liposomes, Biophys. Chem. 95 (2002) 145–155.

[3] R. Stevanato, F. Momo, M. Marian, et al., Effects of nitrosopropofol on mitochondrial energy-converting system, Biochem. Pharmacol. 7384 (2002) 1–6.

[4] H. Tsuchiya, Structure-specific fluidizing effect of propofol, Clin. Exp. Pharmacol. Physiol. 28 (2001) 292–299.

[5] J. Baber, J.F. Ellena, D.S. Cafiso, Distribution of general anaesthetics in phospholipid bilayers determined using $^{2}H$ NMR and $^{1}H–^{1}H$ NOE spectroscopy, Biochemistry 34 (1995) 6533–6539.

[6] J. Miyazaky, K. Hideg, D. Marsh, Interfacial ionization and partitioning of membrane-bound local anaesthetics, Biochim. Biophys. Acta 1103 (1992) 62–68.

[7] A. Anel, G.V. Richieri, A.M. Kleinfeld, Membrane partition of fatty acids and inhibition of T-cell function, Biochemistry 32 (1993) 530–536.

[8] F.J. Aranda, J. Villalain, The interaction of abietic acid with phospholipid membranes, Biochim. Biophys. Acta 1327 (1997) 171–180.

[9] M.S. Kharasch, B.S. Joshi, Reactions of hindered phenols. III. Reaction of nitrous acid with hindered phenols, J. Org. Chem. 27 (1962) 651–653.

[10] Kusumi, W.K. Subczynski, J.S. Hyde, Oxygen transport parameter in membranes as deduced by saturation recovery measurements of spin-lattice relaxation times of spin labels, Proc. Natl. Acad. Sci. USA 79 (1982) 1854–1858.

[11] L.D. Mayer, M.J. Hope, P.R. Cullis, Vescicles of variable sizes produced by a rapid extrusion procedure, Biochim. Biophys. Acta 858 (1986) 161–168.

[12] A.G. Gornall, C.J. Bardwill, M.M. David, Determination of serum proteins by means of the biuret reaction, J. Biol. Chem. 177 (1949) 751–756.

[13] M.K. Jain, N. Min Wu, Effect of small molecules on the dipalmitoyl lecithin liposomal bilayer: III. Phase transition in lipid bilayer, J. Membrane Biol. 34 (1977) 157–201.

[14] Y. Kaminoh, C. Tashiro, H. Kamaya, I. Ueda, Depression of phase transition temperature by anaesthetics: non-zero solid binding, Biochim. Biophys. Acta 946 (1988) 215–220.

[15] J.A. Rogers, S. Davis, Functional group contributions to the partitioning of phenols between liposomes and water, Biochim. Biophys. Acta 598 (1980) 392–404.

[16] D. Marsch, Electron spin resonance: spin labels, in: E. Grell (Ed.), Membrane Spectroscopy, Springer-Verlag, New York, 1981, pp. 51–142.